Ca^{2+}- and mitochondrial-dependent cardiomyocyte necrosis as a primary mediator of heart failure

Hiroyuki Nakayama,[1] Xiongwen Chen,[2] Christopher P. Baines,[1] Raisa Klevitsky,[1] Xiaoying Zhang,[3] Hongyu Zhang,[2] Naser Jaleel,[2] Balvin H.L. Chua,[4] Timothy E. Hewett,[1] Jeffrey Robbins,[1] Steven R. Houser,[2] and Jeffery D. Molkentin[1]

[1]Department of Pediatrics, Cincinnati Children's Hospital Medical Center, University of Cincinnati, Cincinnati, Ohio, USA. [2]Department of Physiology, Temple University School of Medicine, Philadelphia, Pennsylvania, USA. [3]Fox Chase Cancer Center, Philadelphia, Pennsylvania, USA. [4]James H. Quillen School of Medicine, East Tennessee State University, and James H. Quillen Veterans Affairs Medical Center, Johnson City, Tennessee, USA.

Loss of cardiac myocytes in heart failure is thought to occur largely through an apoptotic process. Here we show that heart failure can also be precipitated through myocyte necrosis associated with Ca^{2+} overload. Inducible transgenic mice with enhanced sarcolemmal L-type Ca^{2+} channel (LTCC) activity showed progressive myocyte necrosis that led to pump dysfunction and premature death, effects that were dramatically enhanced by acute stimulation of β-adrenergic receptors. Enhanced Ca^{2+} influx–induced cellular necrosis and cardiomyopathy was prevented with either LTCC blockers or β-adrenergic receptor antagonists, demonstrating a proximal relationship among β-adrenergic receptor function, Ca^{2+} handling, and heart failure progression through necrotic cell loss. Mechanistically, loss of cyclophilin D, a regulator of the mitochondrial permeability transition pore that underpins necrosis, blocked Ca^{2+} influx–induced necrosis of myocytes, heart failure, and isoproterenol-induced premature death. In contrast, overexpression of the antiapoptotic factor Bcl-2 was ineffective in mitigating heart failure and death associated with excess Ca^{2+} influx and acute β-adrenergic receptor stimulation. This paradigm of mitochondrial- and necrosis-dependent heart failure was also observed in other mouse models of disease, which supports the concept that heart failure is a pleiotropic disorder that involves not only apoptosis, but also necrotic loss of myocytes in association with dysregulated Ca^{2+} handling and β-adrenergic receptor signaling.

Introduction

Cardiovascular disease remains the primary cause of mortality in the Western world, with heart failure representing the fastest-growing subclass over the past decade (1–3). There are approximately 5 million Americans currently diagnosed with heart failure, which is characterized by a 5-year survival rate of approximately 50% and which has a total economic impact as high as $100 billion per year (4–6). Typically, heart failure is the culmination of long-standing diseases such as hypertension, ischemia from atherosclerosis, viral myocarditis, valvular insufficiency, or mutations in genes encoding sarcomeric proteins (6, 7). Poor ventricular pump function in heart failure activates reflex pathways that lead to increased catecholamine release within the heart and endocrine tissues in an attempt to maintain adequate perfusion. The persistent activation of these reflex responses appears to hasten the demise of the myocardium, in part through an increase in myocyte death associated with excess catecholamines (7–12). Beneficial cardiac remodeling at the cellular and whole-organ level is promoted by β-adrenergic receptor antagonists, which results in an increase in left ventricular ejection fraction and a significant prolongation in lifespan through mechanisms that are largely unknown (13–15).

Heart failure is also characterized by ventricular dilation, elevated systolic wall stress, dysregulation in Ca^{2+} homeostasis within the myocyte, and activation of the sympathetic nervous system (13–16). To induce ventricular contraction, Ca^{2+} enters cardiomyocytes through the L-type Ca^{2+} channel (LTCC) during the early portion of the action potential, causing the release of a much larger amount of Ca^{2+} from the sarcoplasmic reticulum (SR) storage compartment by activating the ryanodine receptor (17) and thereby causing contraction. Myocyte relaxation is initiated by resequestration of Ca^{2+} into the SR via SR Ca^{2+} ATPase (SERCA2) and by Ca^{2+} efflux via the sarcolemmal Na^+/Ca^{2+} exchanger (NCX). The magnitude and timing of the Ca^{2+} transient determines the strength of contraction and is dynamically regulated by catecholamines binding to β-adrenergic receptors, resulting in the activation of adenylyl cyclase, the generation of cAMP, and the subsequent activation of PKA (17). Once activated, PKA directly phosphorylates nodal Ca^{2+} regulatory proteins such as the LTCC (increased Ca^{2+} influx), the ryanodine receptor (increased SR Ca^{2+} release), and phospholamban (PLN; increased SERCA2 activity) as a means of enhancing total intracellular Ca^{2+} release (17, 18). In the dilated, failing heart, myocytes must generate greater than normal amounts of force to eject blood against a pathologically elevated increase in afterload (systolic wall stress). This requires persistent activation of sympathetic regulatory pathways to augment myocyte Ca^{2+} handling in a PKA-dependent manner. When myocytes are isolated from these failing hearts and taken out of this "sympathetic" context, they show a compensatory prolongation and slowed decay of the Ca^{2+} transient and an inability to effectively remove Ca^{2+} in diastole

Nonstandard abbreviations used: CsA, cyclosporine A; Dox, doxycycline; DTG, double transgenic; Iso, isoproterenol; LTCC, L-type Ca^{2+} channel; α-MHC, α–myosin heavy chain; MPT, mitochondrial permeability transition; NCX, Na^+/Ca^{2+} exchanger; PLN, phospholamban; SERCA2, SR Ca^{2+} ATPase; SR, sarcoplasmic reticulum; TAC, transverse aortic constriction; tTA, tet-transactivator protein.

Conflict of interest: The authors have declared that no conflict of interest exists.

Citation for this article: *J. Clin. Invest.* **117**:2431–2444 (2007). doi:10.1172/JCI31060.

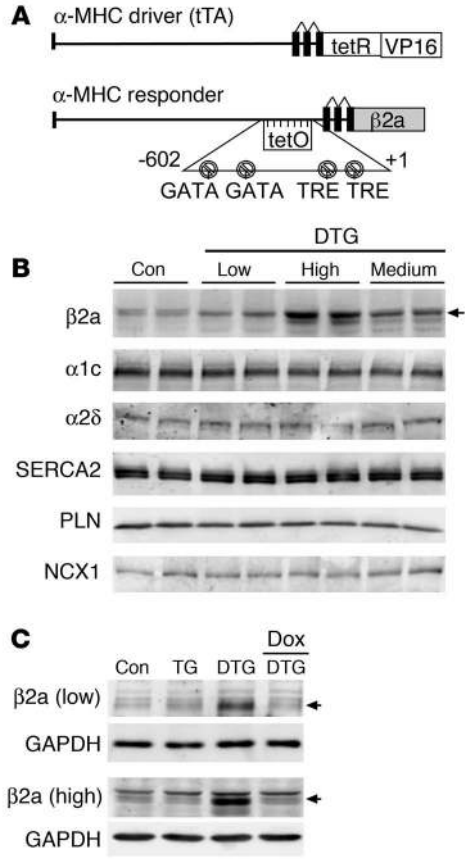

Figure 1
Generation of inducible transgenic mice with increased LTCC activity. (**A**) Schematic of the bitransgenic inducible expression system used to regulate β2a expression in the mouse heart. tetR, tet-repressor cDNA fused to VP16 (activator domain); tetO, tet-operator; TRE, thyroid hormone regulatory element. (**B**) Western blot analysis of β2a protein levels in the heart of low-, medium-, and high-expressing DTG mice raised without Dox (induced state). Levels of α1c, α2δ, SERCA2a, PLN, and NCX1 were unchanged. Con, control tTA single-transgenic mice. (**C**) Western blots showing inducible expression of β2a in low- and high-expressing DTG mice without Dox and its extinguishment with 2–3 weeks of Dox administration. TG, β2a transgene alone (without the driver tTA transgene). Control samples were from tTA single-transgenic mice.

(16, 19). Persistent Ca^{2+} and adrenergic stress in the failing heart is thought to enhance cell death, although this hypothesis has yet to be definitively evaluated in vivo (20).

Alterations in catecholamines and Ca^{2+} handling could promote cardiomyocyte death in heart failure through an apoptotic pathway, a necrotic pathway, or both. Apoptotic cell death is mediated by both an extrinsic pathway, consisting of death receptor signaling constituents, and an intrinsic pathway, consisting of pro-death Bcl-2 family members functioning at the level of the mitochondria and endoplasmic reticulum (21, 22). Countless studies have shown the association and/or causation between the apoptotic loss of myocytes and the progression of heart failure in humans and in animal models (12). While considerably less studied, necrosis may also be a critical mechanism underlying myocyte loss in heart failure or with aging (10, 21). Necrotic cell death is largely initiated at the level of the mitochondria following Ca^{2+} overload, hypoxia, and oxidative damage (22). The mitochondrial permeability transition (MPT) pore, a protein complex that spans the outer and inner mitochondrial membranes, is considered to be the mediator of this event. The MPT has been hypothesized to minimally consist of the voltage-dependent anion channel in the outer membrane, the adenine nucleotide translocase in the inner membrane, and cyclophilin-D in the matrix (23–25). Mitochondrial Ca^{2+} overload following ischemic injury, and possibly in disease states that lead to heart failure, can promote MPT and the induction of necrosis, although the contribution of this process to heart failure has not been evaluated (26–28). This concept is also supported by the observation of focal necrosis in Syrian cardiomyopathic hamsters deficient in δ-sarcoglycan (*Scgd*) through a mechanism that may involve calcium overload (29).

Here we show that enhancement of cardiomyocyte Ca^{2+} influx within the hearts of adult mice through sustained LTCC activation induced cell death through a mitochondrial-dependent necrotic process. This Ca^{2+} overload–dependent necrosis was enhanced or abated by activation or inhibition, respectively, of β-adrenergic receptors. Inhibition of cellular apoptosis by Bcl-2 overexpression in the heart did not diminish Ca^{2+} overload–induced myocyte death or heart failure or affect premature lethality in mice. In contrast, deletion of *Ppif*, which encodes cyclophilin D, blocked Ca^{2+} overload–induced cell death, heart failure, and premature lethality. These results demonstrate that myocyte necrosis can be a significant contributor to heart failure through a β-adrenergic receptor–modulated pathway involving Ca^{2+} overload and MPT.

Results

Generation of mice with inducible LTCC activity. The LTCC is the primary source of Ca^{2+} influx that causes SR Ca^{2+} loading and release in cardiac myocytes. In heart failure the overall activity of the LTCC is likely increased, contributing to a greater profile of Ca^{2+} handling dysfunction (30, 31). Here we generated an inducible transgenic mouse to examine the effects of persistent increases in LTCC activity in the initiation and progression of heart failure. The β2a subunit of the LTCC was selected for overexpression because it enhances channel open probability and increases trafficking of the pore-forming α1c subunit to the sarcolemma, thereby causing greater Ca^{2+} influx (18, 32, 33). A modified α–myosin heavy chain (α-MHC) promoter was used as the responder (34); when crossed with transgenic mice containing the α-MHC promoter–driven tet-transactivator protein (tTA), this produced cardiac-specific expression in the heart that was regulated by doxycycline (Dox) administration and/or withdrawal (Figure 1A). Multiple lines of β2a-containing mice were initially generated, and we selected lines with low (3.1-fold), medium (4.5-fold), and high (7.4-fold) β2a expression for characterization (Figure 1B). Overexpression of β2a did not cause alterations in other components of the LTCC, such as α1c or α2δ, nor were other nodal Ca^{2+} handling proteins altered, in mice at 14 weeks of age (Figure 1B). Most subsequent work was performed in only low- and high-expressing lines for convenience, although medium-expressing mice showed a phenotype that was most similar to the high-expressing line (data not shown). To demonstrate the reliability of the inducible system, Dox was administered to low- and high-expressing lines crossed with the tTA line (double transgenic; DTG), demonstrating a complete extinguishment of β2a overexpression (Figure 1C).

Characterization of Ca^{2+} handling and contractility. Myocytes isolated from young adult high- and low-expressing DTG mice without

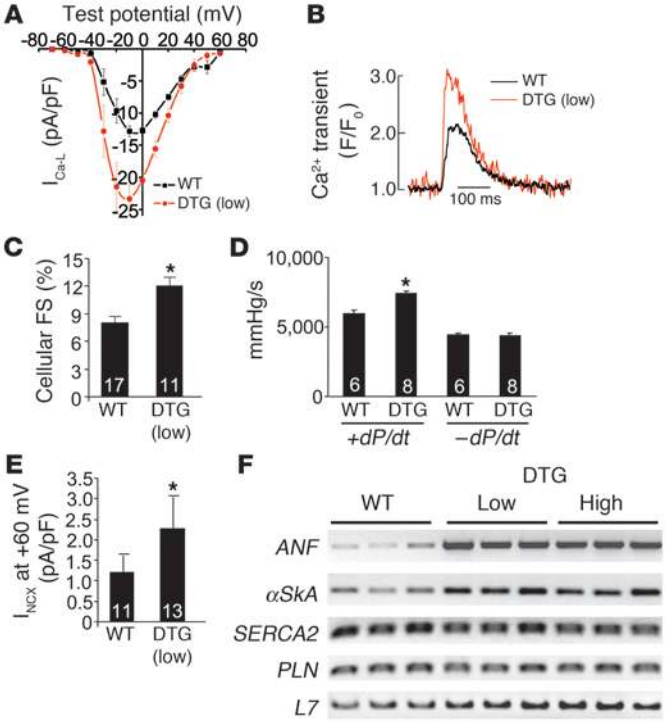

Figure 2
Analysis of Ca^{2+} handling in β2a-inducible transgenic mice. (**A**) Ca^{2+} current (I_{Ca-L}) at different test potentials from adult myocytes isolated from control wild-type mice or low-expressing DTG mice without Dox administration. From 3 independent mice per group, 17 myocytes from control hearts and 11 myocytes from DTG hearts were analyzed. (**B**) Representative Ca^{2+} transients from control wild-type and DTG myocytes measured as a change in fluorescence. (**C**) Assessment of cellular fractional shortening (FS) after isolation from control wild-type and low-expressing DTG mice. Numbers indicate the number of cells analyzed in each group. *$P < 0.05$ versus wild-type, Student's *t* test. (**D**) Isolated working heart preparation to measure ± dP/dt in control wild-type and low-expressing DTG mice at 14 weeks of age. Numbers indicate the number of hearts analyzed in each group. *$P < 0.05$ versus wild-type, Student's *t* test. (**E**) Current associated with NCX activity in adult myocytes isolated from control wild-type and low-expressing DTG mouse hearts. Numbers indicate the number of cells analyzed in each group. *$P < 0.05$ versus wild-type, Student's *t* test. (**F**) RT-PCR for atrial natriuretic factor (*ANF*), skeletal α-actin (*αSkA*), *SERCA2*, *PLN*, or *L7* (control) from hearts of control wild-type mice as well as low- and high-expressing DTG mice ($n = 3$ per group).

Dox administration had significantly larger L-type Ca^{2+} currents, Ca^{2+} transients, and myocyte fractional shortening compared with wild-type controls (Figure 2, A–C, and data not shown). Hearts isolated from young adult low-expressing DTG mice had greater contractility in systole in a working heart preparation, while relaxation was not altered (Figure 2D). The increase in total Ca^{2+} influx observed in DTG mice was associated with a significant increase in NCX activity, the primary mechanism for Ca^{2+} efflux in cardiac myocytes, in isolated myocytes (Figure 2E). There were no changes in *SERCA2* or *PLN* mRNA levels (Figure 2F). Adult myocytes isolated from low-expressing DTG mice showed no significant increase in diastolic calcium at 0.5 Hz stimulation, although at higher stimulation frequencies, DTG myocytes showed higher diastolic calcium levels compared with wild-type control myocytes (data not shown). These experiments showed that inducible overexpression of the β2a subunit of the LTCC increased Ca^{2+} influx and myocyte and cardiac contractility in young mice. However, low- and high-expressing DTG mice showed activation of hypertrophic/stress response genes in the heart, such as atrial natriuretic factor and skeletal α-actin, suggesting that pathology might ensue as the mice aged further (Figure 2F).

Overexpression of β2a induces cardiomyopathy. The analysis of Ca^{2+} current and contractile properties presented above was performed in low-expressing DTG mice at a relatively young age (12–14 weeks), when they had normal or enhanced ventricular function; fibrosis, ventricular dysfunction, and premature lethality became apparent in these mice by 6–12 months of age (Figure 3A). By comparison, high- and medium-expressing DTG mice already showed signs of cardiomyopathy by 12–14 weeks of age.

Hearts from low- and high-expressing DTG mice without Dox administration were hypertrophic by 4 months of age, with significant increases in heart weight normalized to body weight (Figure 3B). Cardiac function, as assessed by echocardiography, was abnormal in high-expressing DTG mice by 4 months of age (Figure 3C) and became dysfunctional in low-expressing DTG mice by 12 months of age (data not shown). Histological assessment of cardiac pathology demonstrated areas of myocyte disorganization and focal and interstitial fibrosis in both low- and high-expressing DTG mice, although these abnormalities were always more pronounced in high-expressing DTG mice (Figure 3, D and E). Approximately 1 of 3 hearts from high-expressing DTG mice at 4 months of age showed areas of myocyte dropout that reacted with the Ca^{2+}-specific von Kossa deposition stain, suggestive of Ca^{2+} overload in these myocytes (Figure 3D, far right panel). Cardiac histological sections left at room temperature (from animals that had expired 8 hours prior) did not react with von Kossa staining, suggesting specificity for Ca^{2+} deposits associated with an active overload process (data not shown). These histological abnormalities were not associated with increased levels of TUNEL staining, suggesting that myocytes were not undergoing apoptosis as a result of increased Ca^{2+} influx (Figure 3F). As an important control, wild-type mice subjected to pressure overload by transverse aortic constriction (TAC) showed a nearly 3-fold increase in TUNEL (Figure 3F) (see Discussion).

Verapamil prevents disease in DTG mice. We examined whether overexpression of the β2a subunit of the LTCC induces disease specifically through increased Ca^{2+} influx by treating high-expressing DTG mice without Dox administration with the LTCC inhibitor verapamil. Mice were given verapamil at weaning (3 weeks of age) and maintained on drug for 14 weeks before analysis. Verapamil-treated high-expressing DTG mice had no hypertrophy and reduced atrial pathology, and cardiac function as assessed by fractional shortening was not diminished (Figure 4, A–C). Verapamil treatment also reduced histopathology and the relative extent of fibrosis and completely prevented histological Ca^{2+} deposits (Figure 4, D and E). These results indicate that the mechanism for β2a

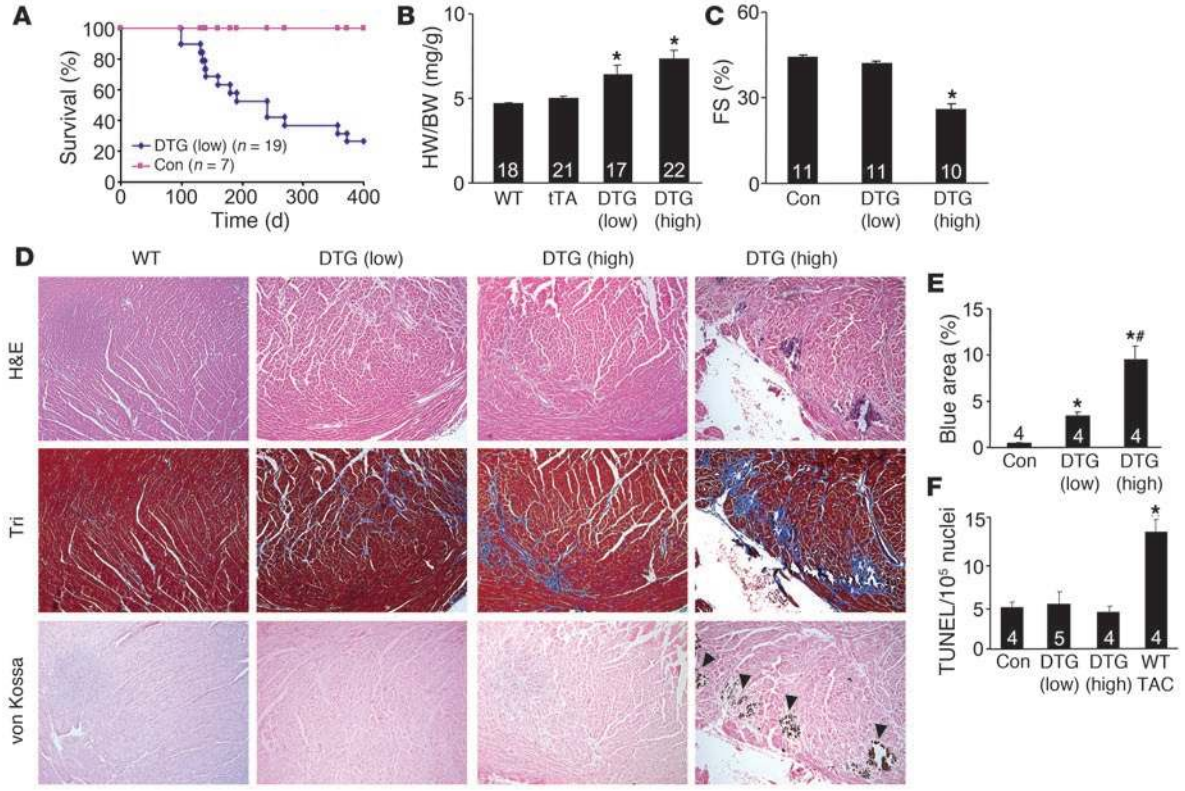

Figure 3
Cardiac phenotype of β2a DTG mice. (**A**) Kaplan-Meier curves of death with aging in control tTA single-transgenic and low-expressing DTG mice. (**B**) Heart weight (HW) normalized to body weight (BW) for control wild-type, tTA single-transgenic, and high- and low-expressing DTG mice at 4 months of age. Numbers indicate the number of mice analyzed in each group. **P* < 0.05 versus wild-type and tTA single-transgenic, Student's *t* test. (**C**) Fractional shortening assessment by echocardiography in the indicated groups. Numbers indicate the number of mice analyzed in each group. **P* < 0.05 versus control, Student's *t* test. (**D**) Histological assessment of cardiac ventricular pathology by H&E, Masson's trichrome (Tri), and von Kossa staining in control wild-type and low- and high-expressing DTG mice. Arrowheads denote regions of von Kossa–detected Ca^{2+} overload. Original magnification, ×100. (**E**) Quantitation of fibrotic area (blue) from trichrome-stained cardiac histological sections. Numbers indicate the number of mouse hearts analyzed in each group. **P* < 0.05 versus control; #*P* < 0.05 versus low-expressing DTG, Student's *t* test. (**F**) Assessment of TUNEL-positive myocyte nuclei from hearts of the indicated mice. Numbers indicate the number of hearts analyzed in each group. **P* < 0.05 versus control, Student's *t* test.

overexpression–induced cardiomyopathy involves increased Ca^{2+} influx through the LTCC.

Synergy of β-adrenergic receptor activity with the LTCC induces Ca^{2+} overload and necrosis. Because β-adrenergic receptor activity augments LTCC and SR activity, it should further increase Ca^{2+} influx and SR Ca^{2+} loading in β2a DTG mice. Infusion of isoproterenol (Iso; 60 mg/kg/d) induced death in all high-expressing DTG mice within 12 days and in 4 of 9 low-expressing DTG mice (Figure 5A). No tTA single-transgenic control mouse showed any lethality at this dosage of Iso, nor did the mice have increased histopathology beyond wild-type mice treated with Iso. The low-expressing DTG mice that survived Iso infusion had significant reductions in ventricular performance, with large areas of myocyte loss and fibrosis (Figure 5, B, C, and E). Remarkably, large areas of myocyte dropout were observed in the ventricular walls and septum of Iso-infused DTG mice (Figure 5C). von Kossa staining showed areas of significant Ca^{2+} deposition in myocytes throughout the ventricular walls and septum that corresponded with regions of focal myocyte necrosis (Figure 5, D and F). However, the number of TUNEL-positive myocytes in these same histological sections was not significantly greater than in control hearts without Iso, suggesting that the widespread and focal loss of myocytes during and after Iso infusion was primarily caused by myocyte necrosis (data not shown). Collectively, these results suggest that β-adrenergic receptor–augmented LTCC activity in β2a mice caused acute Ca^{2+} overload, myocyte necrosis, and premature death.

The pathology associated with β2a overexpression in low- and high-expressing DTG mice was prevented when the inducible transgene was extinguished with Dox administration. For example, high-expressing DTG mice showed no overt pathology, hypertrophy, or reduction in ventricular performance when administered Dox (Figure 6, A–C). Moreover, low-expressing DTG mice challenged with Iso infusion showed almost no lethality when given Dox continuously 2 weeks prior to minipump insertion, which completely extinguished β2a overexpression (Figure 6D). These mice also did not develop cardiac dysfunction (Figure 6E), and histological assessment showed no significant increase in fibrosis or von Kossa–positive myocytes (Figure 6, F and G).

Assessment of cellular necrosis. The focal areas of myocyte loss, fibrosis, and von Kossa–positive myocytes in β2a DTG mice sug-

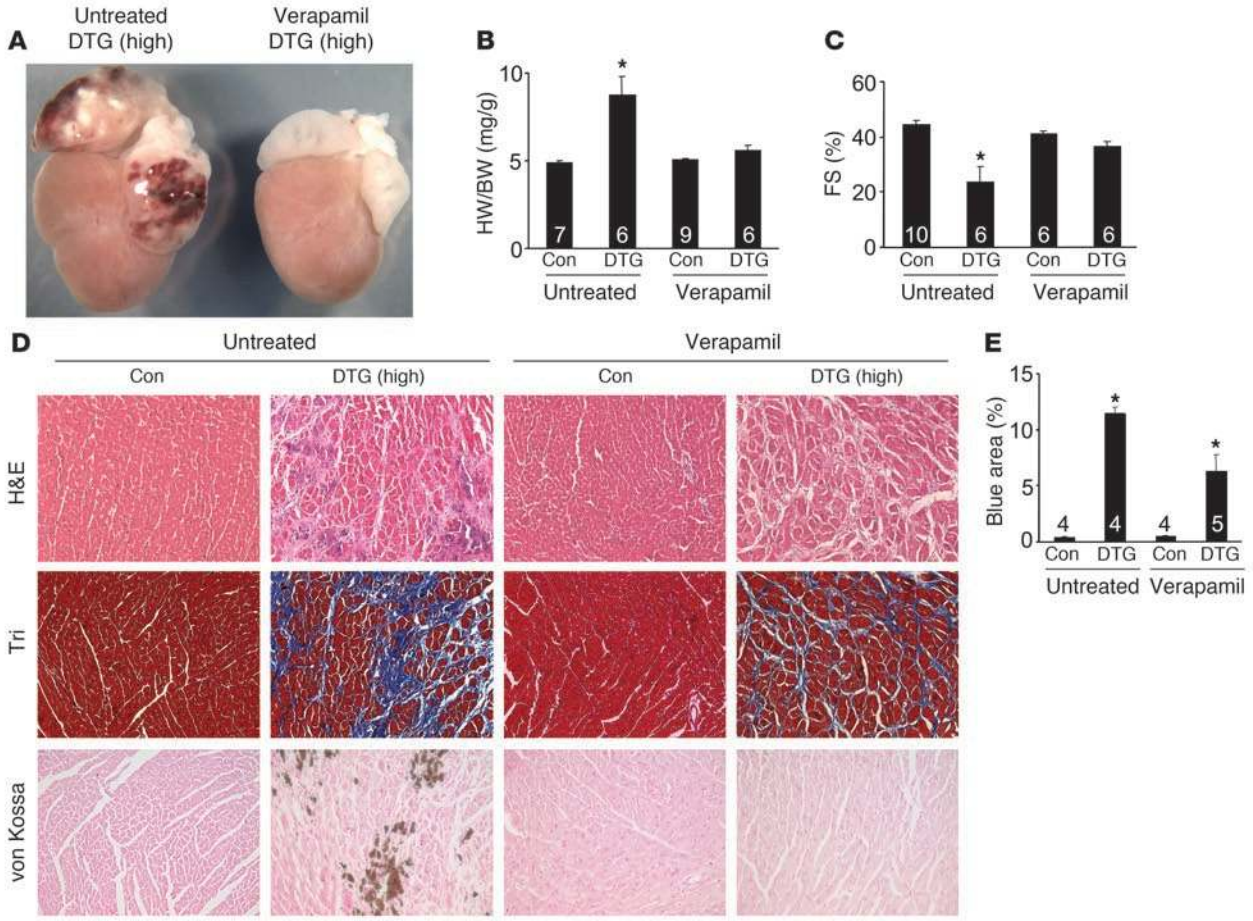

Figure 4

Verapamil reduces cardiac pathology in β2a DTG mice. (**A**) Gross morphological view of hearts from a high-expressing DTG β2a mouse with or without verapamil treatment (4 months of age). (**B**) Heart weight normalized to body weight for control tTA single-transgenic and high-expressing DTG mice with or without verapamil. Numbers indicate the number of mice analyzed in each group. *$P < 0.05$ versus untreated control, ANOVA. (**C**) Fractional shortening assessment by echocardiography in control tTA single-transgenic and high-expressing DTG mice with or without verapamil. Numbers indicate the number of mice analyzed in each group. *$P < 0.05$ versus untreated control, ANOVA. (**D**) Histological assessment of cardiac ventricular pathology by H&E, Masson's trichrome, and von Kossa staining in control tTA single-transgenic and high-expressing DTG mice with or without verapamil. Original magnification, ×200. (**E**) Quantitation of fibrotic area (blue) from trichrome-stained cardiac histological sections. Numbers indicate the number of sections analyzed in each group. *$P < 0.05$ versus control, ANOVA.

gested a cellular phenotype of necrosis, but not apoptosis. Indeed, in addition to no increase in TUNEL (Figure 3), DTG mice also failed to show significant increases in caspase 3 cleavage in the heart at baseline or after acute Iso infusion (data not shown). However, assessment of necrosis using the myosin antibody injection technique showed detectable levels of basal necrosis in the hearts of low-expressing DTG mice without stimulation (5 cells per 10,000), yet no reactivity was observed in control mice (Figure 7, A and B) (21). Acute infusion of Iso caused a massive increase in necrotic myosin-positive cells in DTG mice, compared with a small effect in control mice (Figure 7, A and B). The baseline increase in necrosis in DTG mice was also associated with a small, albeit significant, increase in myeloperoxidase activity in the heart that was associated with increased granulocyte content that typically occurs with necrosis (Figure 7C).

We previously observed an increase in cell death in cultured adult feline ventricular myocytes overexpressing the same β2a subunit of the LTCC (35). Loss of β2a-dependent cells (adenoviral gene transfer) showed indexes of both apoptotic and necrotic cell death, although the relatively unphysiologic context associated with culturing precludes a rigorous assignment of the exclusivity between apoptotic and necrotic mechanisms (35). Here we extended these observations to show that very low levels of β-adrenergic receptor stimulation (Iso, 10^{-9} M) synergized with β2a overexpression to induce myocyte death (Figure 7, D and E). This dose of Iso had no effect on control-infected myocytes without β2a overexpression (Figure 7, D and E). Moreover, this synergistic increase in cell death was partially blocked (about 50% recovery; $P < 0.05$) with cyclosporine A (CsA), which can antagonize MPT associated with calcium overload (data not shown). These results are consistent with our in vivo observations suggesting that myocyte calcium overload in conjunction with β-adrenergic receptor stimulation can lead to rapid cell death.

Blockade of β-adrenergic receptors prevents disease in DTG mice. The interplay between β-adrenergic receptors and LTCC activity as a primary determinant of Ca^{2+} overload–induced cell death and cardio-

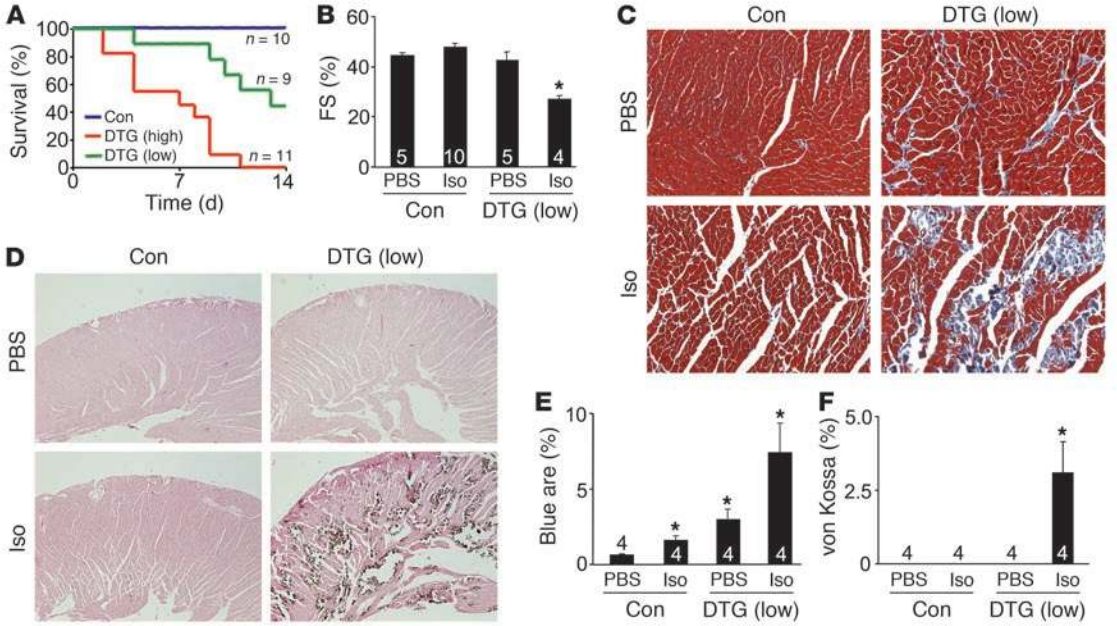

Figure 5

Iso infusion dramatically enhances β2a-dependent disease and death. (**A**) Kaplan-Meier curves of control tTA single-transgenic as well as low- and high-expressing DTG mice infused with Iso at 60 mg/kg/d for 14 days. (**B**) Fractional shortening assessment by echocardiography in control tTA single-transgenic and low-expressing DTG mice with Iso or PBS treatment. Only low-expressing DTG mice were used because 44% survived the 14 days of Iso treatment. Numbers indicate the number of mice analyzed in each group. *$P < 0.05$ versus control with PBS, ANOVA. (**C**) Histological assessment of cardiac ventricular pathology by Masson's trichrome in control tTA single-transgenic and low-expressing DTG mice with Iso or PBS infusion for 14 days. (**D**) Histological assessment of Ca^{2+} deposits in myocytes by von Kossa staining in control tTA single-transgenic and low-expressing DTG mice with Iso or PBS infusion for 14 days. Original magnification, ×200 (**C**); ×40 (**D**). (**E**) Quantitation of fibrotic area (blue) from trichrome-stained cardiac histological sections. Numbers indicate the number of mice analyzed in each group (10 photographs quantified per mouse heart). *$P < 0.05$ versus PBS-infused control, ANOVA. (**F**) Quantitation of areas of myocytes with Ca^{2+} deposits in control tTA single-transgenic and low-expressing DTG mice with Iso or PBS infusion for 14 days. *$P < 0.05$ versus PBS-infused DTG, Student's *t* test.

myopathy was further investigated using a β-adrenergic receptor antagonist. High-expressing DTG mice without Dox administration were given metoprolol at weaning for a 3-month period before being analyzed. Remarkably, metoprolol prevented overt ventricular and atrial hypertrophy, prevented increased heart weight normalized to body weight, and prevented the cardiac dysfunction that was normally observed in high-expressing DTG mice (Figure 8, A–C). Histological analysis also showed a remarkable improvement in fibrosis and areas of myocyte dropout with metoprolol treatment (Figure 8, D and E). These results suggest that inhibition of β-adrenergic receptors reduced disease associated with increased β2a expression by antagonizing the overall Ca^{2+} overload phenomenon itself, likely at multiple levels (see Discussion).

Bcl-2 overexpression does not prevent β2a-dependent Ca^{2+} overload and cardiomyopathy. Overexpression of the antiapoptotic protein Bcl-2 in the heart was previously shown to dramatically attenuate ischemia-reperfusion injury and some forms of cardiomyopathy by directly reducing cardiomyocyte apoptosis (36–38). Thus, the Bcl-2 transgene can serve as an indicator of apoptotic-dependent cardiomyopathy. The Bcl-2 transgene was crossed into the high-expressing DTG background to assess the contribution of apoptosis to the development of β2a-dependent cardiomyopathy. However, no prevention of disease was observed in β2a mice with the Bcl-2 transgene at any age. For example, ventricular and atrial enlargement, reduction in fractional shortening, and histopathology and fibrosis were all identical between high-expressing DTG mice and DTG mice that also contained the Bcl-2 transgene (Figure 9, A–E). Moreover, high-expressing DTG mice with the Bcl-2 transgene showed complete lethality with 14 days of Iso infusion (Figure 9F), similar to DTG mice without the Bcl-2 transgene (Figure 5A). Importantly, overexpression of the β2a subunit did not affect Bcl-2 expression levels driven from this transgene (Figure 9G). Thus, attenuation of apoptotic cell loss with the Bcl-2 transgene did not prevent or reduce disease associated with increased LTCC activity, suggesting that Ca^{2+} overload induces cell loss and cardiomyopathy somewhat independent of apoptosis, at least in the high-expressing β2a line.

Loss of cyclophilin D prevents disease in DTG mice. We have previously shown that loss of *Ppif*, which encodes cyclophilin D, renders cells less sensitive to Ca^{2+} overload–induced necrosis (26). Indeed, $Ppif^{-/-}$ mice have 40% less overall cell loss in the heart following ischemia-reperfusion injury (26). Here we crossed β2a DTG mice into the $Ppif^{-/-}$ background to investigate the centrality of necrosis in the ensuing myocyte loss and cardiomyopathy associated with Ca^{2+} overload. Remarkably, loss of *Ppif* prevented disease associated with the β2a DTG phenotype. For example, DTG mice lacking *Ppif* showed no ventricular or atrial enlargement, no reductions in fractional shortening, and much fewer histological abnormalities such as fibrosis and myocyte dropout (Figure 10, A–E). We were also unable to identify von Kossa–positive myocytes in DTG mice lacking *Ppif*, while DTG controls in the same background showed Ca^{2+} deposits (data not shown). Furthermore, 14 days of

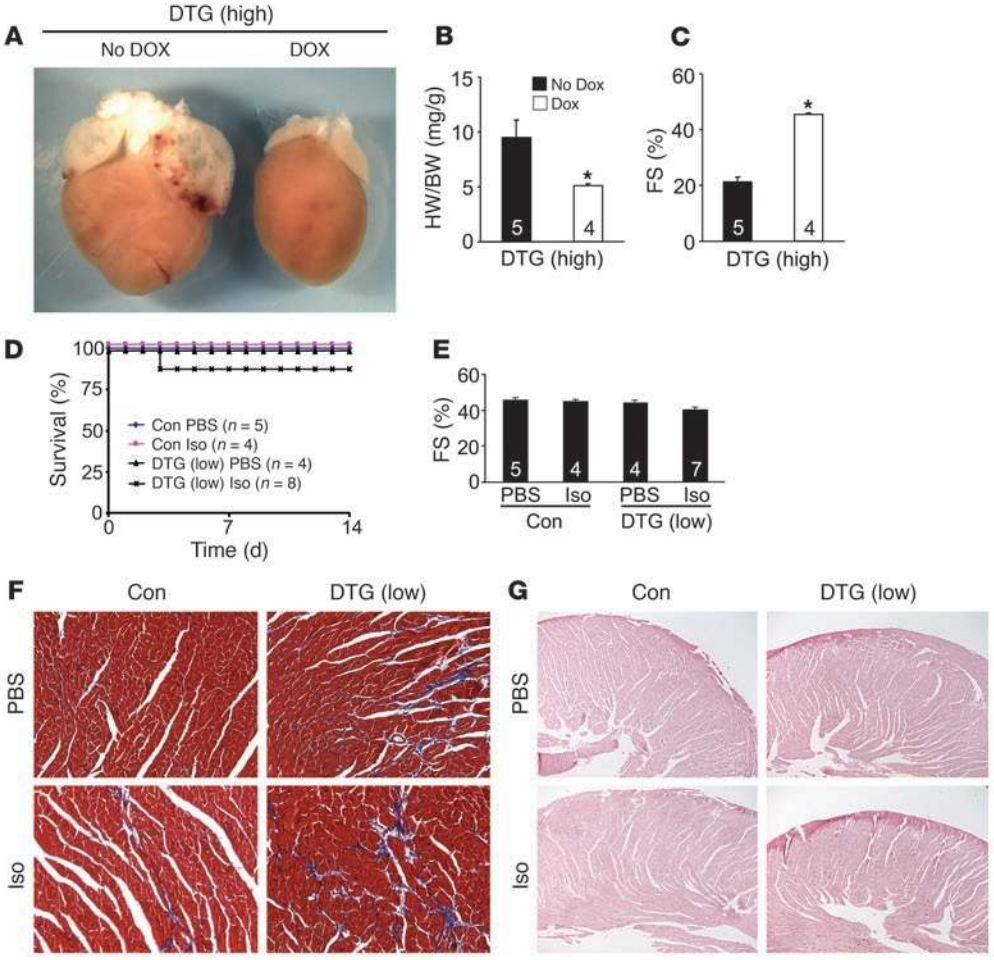

Figure 6

Dox-induced shut-off of the β2a transgene prevents disease. (**A**) Gross morphological pictures of high-expressing DTG β2a mice without Dox treatment (No Dox; induced) or with Dox (shut off) at 14 weeks of age. (**B**) Heart weight normalized to body weight and (**C**) fractional shortening in high-expressing DTG mice without Dox or with Dox. Numbers indicate the number of mice analyzed in each group. *$P < 0.05$ versus DTG without Dox, Student's *t* test. (**D**) Kaplan-Meier curves of control tTA single-transgenic and low-expressing DTG mice infused with Iso at 60 mg/kg/d for 14 days or with PBS vehicle. Low-expressing DTG mice were given Dox for 2 weeks prior to shut off β2a expression. (**E**) Fractional shortening in control tTA single-transgenic and low-expressing DTG mice pretreated with Dox for 2 weeks; some were given 14 days of Iso treatment. Numbers indicate the number of mice analyzed in each group. Data were analyzed by ANOVA. (**F**) Histological assessment of cardiac ventricular pathology by Masson's trichrome in control tTA single-transgenic and low-expressing DTG mice with PBS or Iso infusion for 14 days with 2 weeks of prior Dox treatment. (**G**) Histological assessment of Ca^{2+} deposits in myocytes by von Kossa staining in control tTA single-transgenic and low-expressing DTG mice with PBS or Iso infusion for 14 days with 2 weeks of prior Dox treatment.

Iso infusion produced no lethality in DTG mice in the absence of *Ppif*, while DTG mice from the same cross containing *Ppif* showed identical lethality to other groups of DTG mice discussed above (Figure 10F). As an important control, $Ppif^{-/-}$ mice with the β2a DTG configuration showed the same augmentation in L-type Ca^{2+} current as did β2a DTG mice with 2 good copies of *Ppif* (Figure 10G). These results indicate that inhibition of MPT prevents Ca^{2+} overload–induced disease associated with increased LTCC activity and β-adrenergic receptor signaling (see Discussion).

Assessment of necrotic cell loss in other mouse models of disease. Because overexpression of β2a as a means of inducing heart failure is somewhat arbitrary (although it reveals the underlying pathophysiology of the pathway), we investigated other mouse models of heart failure for signs of mitochondrial-dependent necrosis. Interestingly, the cardiomyopathic hamster lacking *Scgd* showed disease that was associated with enhanced LTCC density and focal necrosis in the heart (29). Serendipitously, we have already crossed $Ppif^{-/-}$ mice with $Scgd^{-/-}$ mice, resulting in a near-complete rescue of focal fibrosis and ventricular performance, which are both normally compromised in this mouse model of muscular dystrophy (D.P. Millay and J.D. Molkentin, unpublished observations). This suggests that muscular dystrophy, which is known to promote an unstable membrane and more Ca^{2+} influx, may also result from a progressive loss of myocytes through a necrotic process.

Experimentally, we also examined antecedents of necrotic cell loss by performing von Kossa staining in hearts from either FVB mice or C57BL/6 mice subjected to long-term pressure overload by TAC. Interestingly, FVB mice are known to be resistant to TAC-induced dysfunction and showed no von Kossa–positive myocytes. However, C57BL/6 mice after only 4 weeks of TAC showed reduced ventricular performance and areas of focal von Kossa–positive myocytes (Figure 11A). In contrast, heart failure associated with disruption of the gene encoding muscle lim protein (*Mlp*) showed no Ca^{2+} accumulation in the heart, suggesting that this model may be independent of a necrotic process (Figure 11A). As a final model, we also subjected mice to doxorubicin treatment, a chemotherapeutic agent that can induce heart failure associated with ROS generation and the accumulation of fibrosis and myocyte dropout. As expected, control mice treated with doxorubicin showed histopathology and reduced ventricular performance 2 weeks later, while $Ppif^{-/-}$ mice were largely protected and showed no histopathology or a reduction in ventricular performance after treatment (Figure 11, B and C). Thus, at least 3 different mouse models of cardiomyopathy and/or heart failure may involve a mitochondrial-dependent necrotic mechanism.

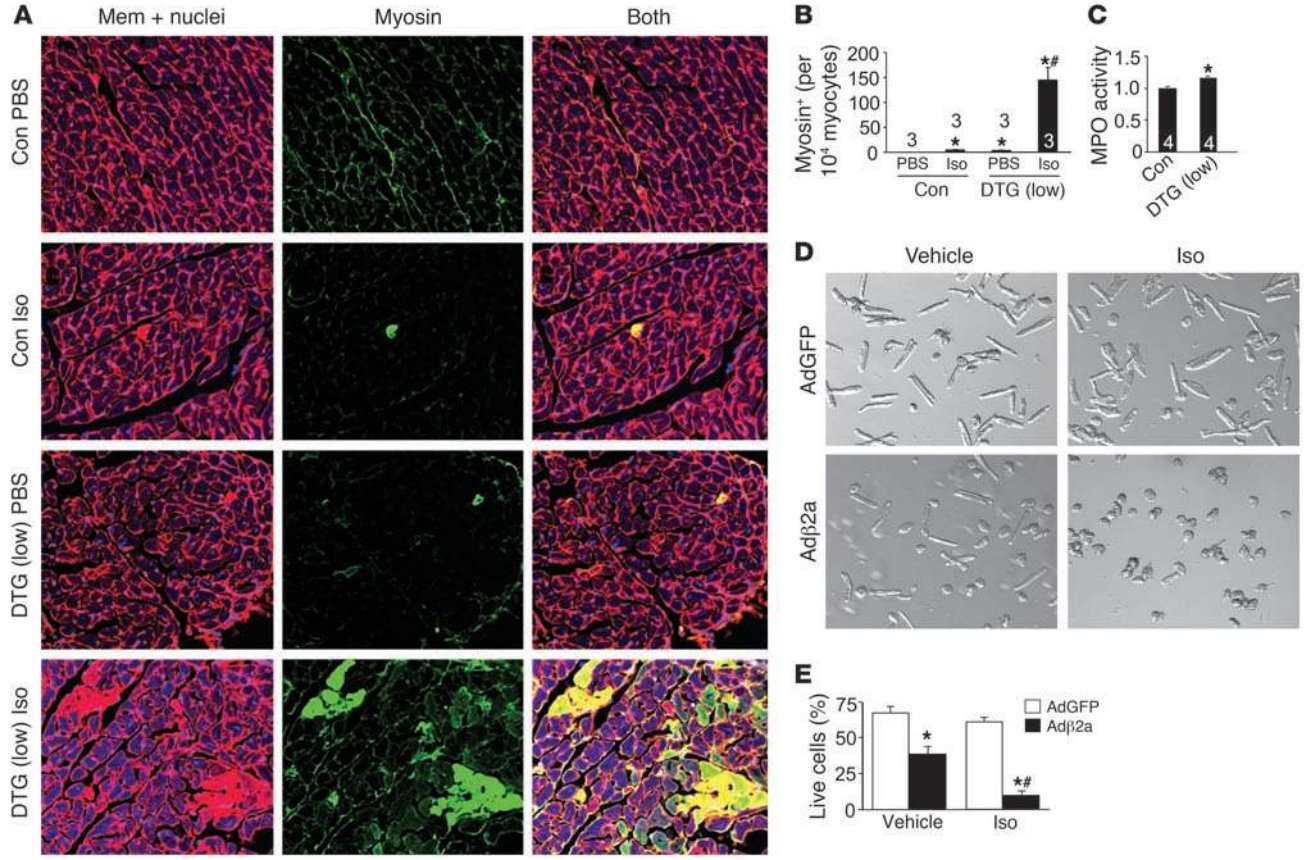

Figure 7

Assessment of myocyte necrosis. (**A**) Immunohistochemistry for myosin antibody incorporation into the heart (green) in control tTA single-transgenic and low-expressing DTG mice with PBS vehicle or Iso infusion for 24 hours. Red is a wheat germ agglutinin stain (TRITC conjugated) for cell membranes (Mem); nuclei are shown in blue. (**B**) Percentage of cells with myosin antibody infiltration per 10,000 myocytes counted. Numbers indicate the number of mice analyzed in each group. $^{*}P < 0.05$ versus PBS-infused control; $^{\#}P < 0.05$ versus Iso-infused control, ANOVA. (**C**) Myeloperoxidase (MPO) activity in hearts that were first perfused to remove any blood contamination and then assayed. Control was arbitrarily set to a value of 1. Numbers indicate the number of mice analyzed in each group. $^{*}P < 0.05$ versus control, Student's *t* test. (**D**) Cultured adult feline ventricular myocytes infected with the indicated recombinant adenoviruses (Ad) and treated with vehicle or Iso. (**E**) Cells in **D** were quantified as the percentage of living rod-shaped cells ($n = 4$ experiments). $^{*}P < 0.05$ versus AdGFP; $^{\#}P < 0.05$ versus vehicle-infused Adβ2a. Original magnification, ×400 (**A**); ×100 (**D**).

Discussion

The observations made here suggest a unique signaling mechanism underlying heart failure that is induced by persistent increases in Ca^{2+} influx through the LTCC, activation of β-adrenergic receptors, and cellular necrosis. To our knowledge, it has not been directly demonstrated before that Ca^{2+} influx–induced myocyte necrosis might be a significant contributor to heart failure, although a number of lines of indirect evidence support this overall hypothesis. Changes in the amount of Ca^{2+} within adult ventricular myocytes needed to alter contractility are primarily accomplished by increasing LTCC-mediated Ca^{2+} fluxes across the sarcolemma. Physiologically, transient increases in cardiac function during exercise occur via catecholamine-regulated increases in Ca^{2+} influx through the LTCC, which increases SR Ca^{2+} loading, the magnitude of the Ca^{2+} transient, and cardiac contractility (39). In the new steady state this increased Ca^{2+} influx and SR Ca^{2+} loading is balanced by increased Ca^{2+} efflux via the NCX or by the plasma membrane Ca^{2+} ATPase pump (39). However, if Ca^{2+} influx is persistently activated or if Ca^{2+} removal systems are persistently compromised, as can occur in heart failure (40), dysfunctional Ca^{2+} handling can induce Ca^{2+} overload. Indeed, loss of the gene encoding NCX1, which removes the protein primarily responsible for Ca^{2+} efflux in cardiac myocytes, results in cardiomyopathy, premature lethality in adulthood, and increased diastolic Ca^{2+} in embryonic heart tubes (41, 42). Abnormal diastolic Ca^{2+} handling can increase diastolic tension by activation of contractile proteins, thus negatively affecting ventricular filling and myocardial energetics, but our present study suggests it may also predispose myocytes to mitochondrial dysfunction and premature death.

We largely expected that β2a overexpression would induce cardiomyopathy since a mouse model with α1c overexpression (pore forming subunit of the LTCC) in the heart was reported to develop disease later in life (43), and based on our earlier observations in β2a adenoviral-infected feline myocytes in culture (35). Indeed, destabilization of the sarcolemmal membrane in *mdx* mice, a model of muscular dystrophy, is associated with increased Ca^{2+} influx and cardiac dysfunction (44), and the hamster model of muscular dystrophy associated with *Scgd* deficiency showed focal necrosis in the

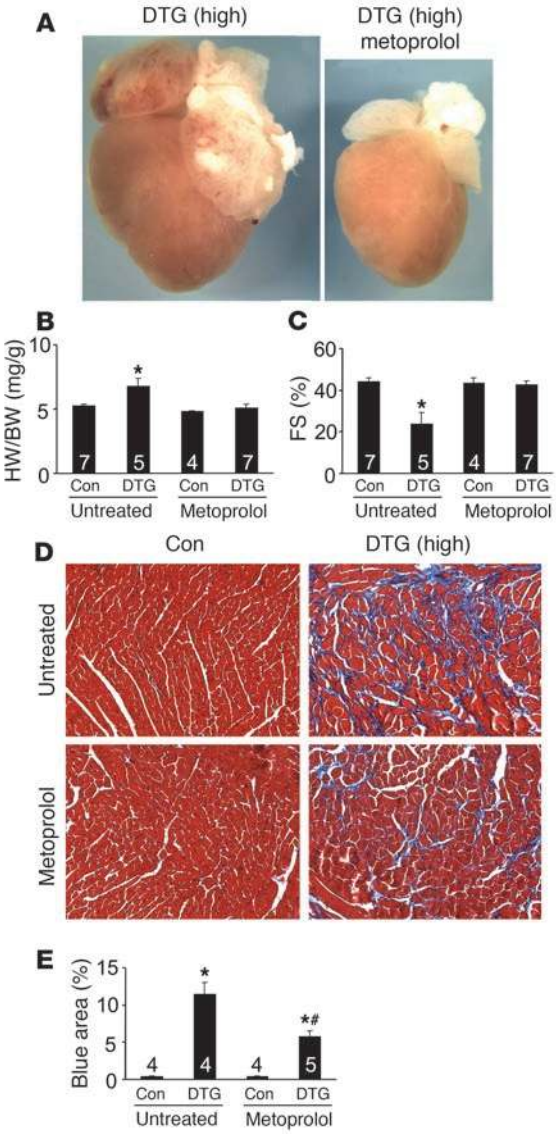

Figure 8
Blocking β-adrenergic receptor prevents disease in high-expressing DTG mice. (**A**) Gross morphological view of hearts from high-expressing DTG β2a mice (4 months of age) with or without metoprolol treatment. (**B** and **C**) Heart weight normalized to body weight (**B**) and fractional shortening assessment (**C**) for control tTA single-transgenic and high-expressing DTG mice with or without metoprolol. Numbers indicate the number of mice analyzed in each group. $^{*}P < 0.05$ versus untreated control, ANOVA. (**D**) Histological assessment of cardiac ventricular pathology by Masson's trichrome staining in the indicated mice. Original magnification, ×200. (**E**) Quantitation of fibrotic area (blue) from trichrome-stained cardiac histological sections. Numbers indicate the number of sections analyzed in each group. $^{*}P < 0.05$ versus untreated control; $^{\#}P < 0.05$ versus DTG without metoprolol, ANOVA.

heart (29). Expression of transient receptor potential channels also promoted greater Ca^{2+} influx and cardiomyopathy (45, 46). In heart failure, PKA- or calmodulin-dependent protein kinase II–dependent phosphorylation of ryanodine receptor is thought to induce triggered arrhythmias via abnormal SR Ca^{2+} release and contractile dysfunction related to diastolic SR Ca^{2+} leak (47–49). Collectively, there is ample support for the link between dysregulated myocyte Ca^{2+} handling and cardiomyopathy and/or heart failure.

However, increased Ca^{2+} cycling within the mouse heart at the level of the SR itself does not induce cardiomyopathy. For example, deletion of *Pln* in the mouse increases SERCA2 activity, resulting in faster Ca^{2+} clearance in diastole, greater Ca^{2+} transients in systole, and enhanced contractility, but no cellular or organ dysfunction (50). Why $Pln^{-/-}$ mice do not develop cardiac dysfunction while the β2a mice studied here had profound cardiac abnormalities is not entirely clear, but could be related to adaptive reductions in Ca^{2+} influx through the LTCC or increases in Ca^{2+} efflux via the NCX. These adaptive changes in Ca^{2+} handling could lead to a scenario in which the enhanced SERCA2 activity in $Pln^{-/-}$ mice produces total cytosolic Ca^{2+} levels averaged across systole and diastole that are not appreciably different from wild type (39). However, human heart failure is characterized by increased LTCC activity (30, 31) and prolongation in the action potential (16), states that tend to increase Ca^{2+} influx. This situation is probably made worse by the fact that SR function is altered in heart failure, with increased diastolic Ca^{2+} leak and dysregulated β-adrenergic receptor function (51).

Further support for altered Ca^{2+} influx as a proximal cause of heart failure comes from studies in the αMHC403/+ mouse model of hypertrophic cardiomyopathy. Isolated myocytes from αMHC403/+ mice showed augmented diastolic Ca^{2+} concentrations that could be made even more pathologic if provoked with inappropriate pharmacologic agents, which induced even greater pathology and death when these same agents were administered in vivo (52). However, alterations in diastolic Ca^{2+} concentrations and ensuing cardiomyopathy in αMHC403/+ mice was prevented with an LTCC antagonist, suggesting another mouse model of disease that results from altered Ca^{2+} influx and possibly enhanced cellular attrition through necrosis (52, 53).

The progression of heart failure in humans is directly influenced by increased systolic wall stress and the activity of β-adrenergic receptors. For example, when cardiac pump function is reduced following an injury, such as after a myocardial infarction, sympathetic reflex responses maintain cardiac pump function and cardiac output by increasing contractility (increased Ca^{2+}) in the surviving myocytes. While initially compensatory, prolonged increases in catecholamines, or supplementation with inotropes that function at the level of the β-adrenergic receptor or cAMP, enhance the progression of heart failure and can lead to cell loss (7–11). Indeed, pharmacologic blockade of β-adrenergic receptors in heart failure provides a significant benefit to patient survival, demonstrating the largely deleterious role associated with constitutively high β-adrenergic receptor signaling in the heart (13–15). It is well established that acute signaling through both β1- and β2-adrenergic receptors result in PKA-mediated phosphorylation of nodal Ca^{2+} handling proteins, leading to augmentation in the Ca^{2+} transient and contractility. It is less certain that β-adrenergic receptors promote heart failure progression through a Ca^{2+}-dependent mechanism, given their prominent desensitization over time. However, a reasonable case can be made that a primary disease mechanism in heart failure is constitutively increased catecholamine levels and β-adrenergic receptor signaling. For example, overexpression of the β1-adrenergic receptor in the hearts of transgenic mice, or high levels of β2-adrenergic receptor expression, eventually induced heart failure with abundant fibrosis (54–58). That Ca^{2+} serves as a pri-

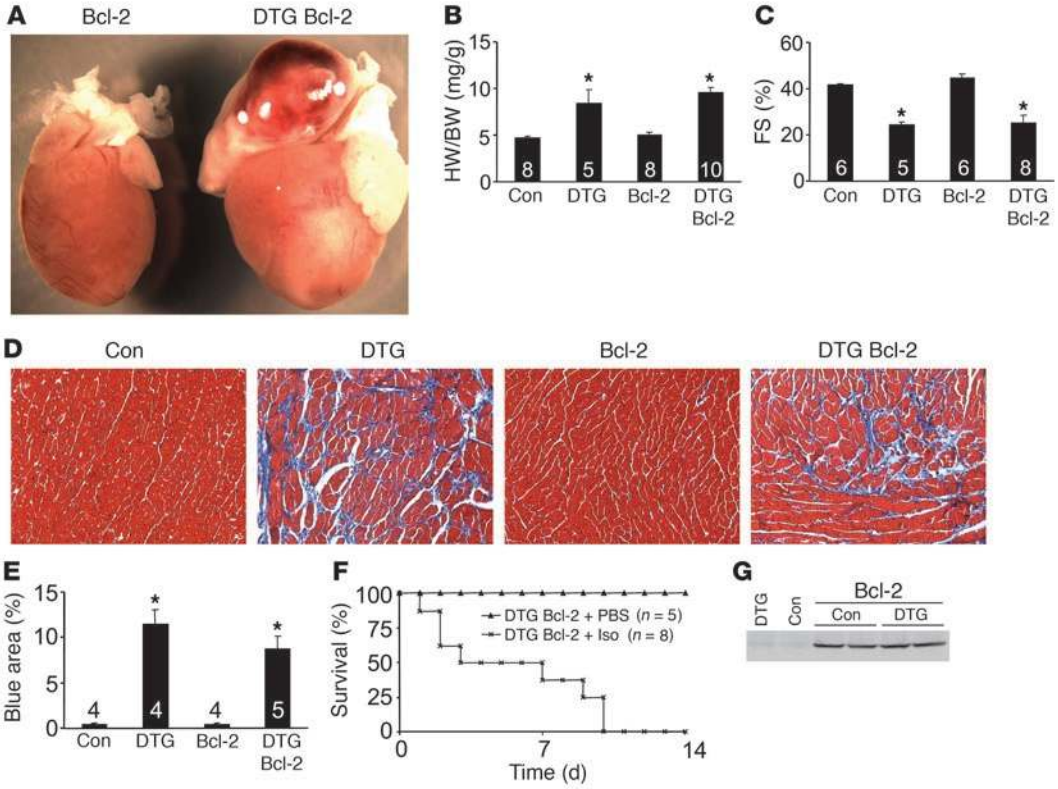

Figure 9

Bcl-2 overexpression does not rescue β2a overexpression–dependent disease. (**A**) Gross morphological view of hearts from a Bcl-2 single-transgenic mouse and a mouse with both the Bcl-2 transgene and the β2a double transgenes without Dox (4 months of age). (**B**–**E**) Heart weight normalized to body weight (**B**), fractional shortening assessment (**C**), histological assessment of cardiac pathology by Masson's trichrome staining (**D**), and quantitation of fibrotic area (blue) from trichrome-stained cardiac sections (**E**) for control tTA single-transgenic mice, DTG mice, Bcl-2 single-transgenic mice, and DTG mice with the Bcl-2 transgene. Numbers indicate the number of mice analyzed in each group (**E**, 10 photographs each). Original magnification, ×200 (**D**). *$P < 0.05$ versus control, ANOVA. (**F**) Kaplan-Meier curves from DTG mice containing the Bcl-2 transgene infused with Iso at 60 mg/kg/d for 14 days or with PBS. (**G**) Western blot for Bcl-2 protein from the hearts of control tTA single-transgenic and DTG mice. GAPDH protein levels did not vary between samples (not shown).

mary effector of β-adrenergic receptor–induced heart failure was demonstrated by a rescue of disease associated with β1-adrenergic receptor overexpression through simultaneous deletion of the *Pln* gene (59). This result suggests that simple removal of diastolic Ca^{2+} caused by enhanced β-adrenergic receptor signaling was sufficient to abate heart failure. This result also suggests that while β-adrenergic receptors may be desensitized in heart failure, they contain sufficient functional capacity to promote Ca^{2+} overload and enhance heart failure progression (19). Our results also support a critical role for β-adrenergic receptors in further augmenting a pathologic profile of Ca^{2+} overload, which likely occurs at the level of the SR (ryanodine receptor) and sarcolemma (LTCC). Indeed, β-adrenergic receptor blockade prevented heart failure in our high-expressing DTG mice.

Heart failure is a complex and progressive syndrome that often culminates in death by arrhythmias or hemodynamic instability. One significant mechanism underlying its progressive nature is a stochastic loss of cardiac myocytes that eventually renders the heart with too few cells to properly function (11, 12). This cumulative loss of myocytes in heart failure has been generally attributed to an apoptotic process (12), suggesting the use of pharmacologic agents that antagonize apoptotic effector proteins such as caspases, pro-death Bcl-2 family members, or nucleases (60). Indeed, alterations in Ca^{2+}, either global or within select microenvironments, can activate Ca^{2+}/calmodulin-dependent kinase in the heart and lead to further alterations in Ca^{2+} handling that can induce myocyte apoptosis and heart failure (61–64). However, essentially no mechanistic data exist implicating a necrotic process of cell loss as a significant contributor to heart failure, although correlative data have been shown. Necrosis occurs in most tissues following ischemic injury or Ca^{2+} overload in combination with depletion of high-energy phosphates such as ATP, resulting in mitochondrial swelling and rupture (22–24). Necrosis associated with mitochondrial swelling and rupture is not thought to be a strictly passive process, but instead can be regulated at the level of the MPT pore through the activity of cyclophilin D (23–25). Disruption of *Ppif* significantly desensitized cells and tissues to necrotic cell death following hypoxia, Ca^{2+} overload, and ROS stimulation in the heart and brain (26–28). Indeed, doxorubicin-induced cardiomyopathy, which involves high levels of ROS as the disease-inducing mechanism, was prevented in *Ppif*$^{-/-}$ hearts. Moreover, enhanced Ca^{2+} influx associated with muscular dystrophy in *Scgd*$^{-/-}$ mice was also partially blocked by deletion of *Ppif* (D.P. Millay and J.D. Molkentin, unpublished observations). There is also evidence that ROS may be even more potent than calcium overload in causing MPT as an underlying determinant of necrotic cell loss in adult myocytes (65).

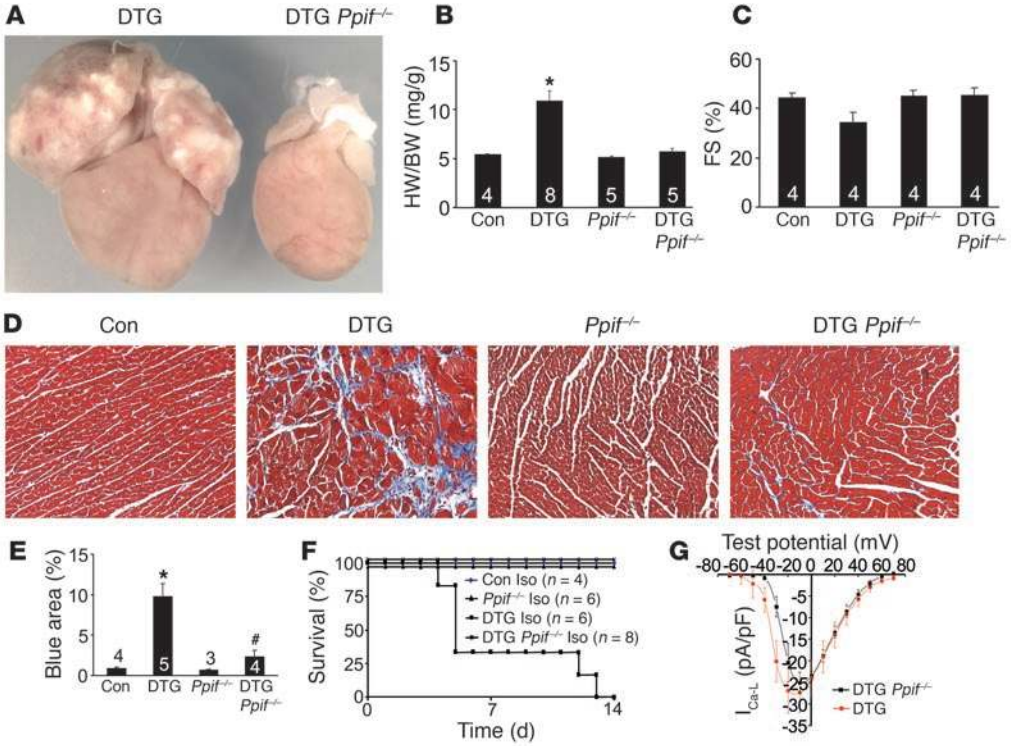

Figure 10

Loss of cyclophilin D rescues disease in β2a-overexpressing mice. (**A**) Gross morphological view of hearts from a DTG mouse and a DTG mouse lacking *Ppif* without Dox (4 months of age). (**B**–**E**) Heart weight normalized to body weight (**B**), fractional shortening assessment (**C**), histological assessment of cardiac pathology by Masson's trichrome staining (**D**), and quantitation of fibrotic area (blue) from trichrome-stained cardiac histological sections (**E**) for control tTA single-transgenic, DTG, *Ppif*$^{-/-}$, and DTG *Ppif*$^{-/-}$ mice. Numbers indicate the number of mice analyzed in each group (**E**, 10 photographs each). Original magnification, ×200 (**D**). $^{*}P < 0.05$ versus control; $^{\#}P < 0.05$ versus DTG, ANOVA. (**F**) Kaplan-Meier curves from control tTA single-transgenic mice, *Ppif*$^{-/-}$ mice, and DTG mice with or without *Ppif* infused with Iso at 60 mg/kg/d for 14 days. (**G**) Ca^{2+} current at different test potentials from adult myocytes isolated from DTG mice ($n = 9$) or DTG *Ppif*$^{-/-}$ mice ($n = 8$). Both show equivalently high currents compared with control wild-type cells shown in Figure 2A.

Regardless of the stimulus, the cumulative loss of cells by necrosis has been correlated with heart failure and aging in a number of previous studies (10, 21). *Ppif*$^{-/-}$ mice may serve as a critical tool for parsing the mechanistic associations between cellular necrosis and heart failure propensity in additional mouse models of disease. Such data might suggest the most appropriate treatments for certain types of heart disease through antinecrotic, antiapoptotic, or a combination of both therapeutic agents for slowing or halting the progression of cellular attrition in heart failure. Inhibition of cyclophilin D can be instituted with CsA, which was shown to potently block MPT many years ago through its interaction with this cyclophilin. However, CsA also inhibits calcineurin as a complex with cyclophilin A, causing a number of other effects in myocytes, some of which may not be desirable. For example, loss of calcineurin activity enhances apoptotic cell loss in the heart (66). Thus, more recent CsA analogs that do not inhibit calcineurin might be advantageous for attenuating MPT and the loss of cells by necrosis in select forms of heart failure.

Methods

Generation of transgenic mice and animal procedures. A cDNA encoding the rat LTCC β2a subunit (35) was cloned into the modified murine α-MHC promoter expression vector to permit Dox-regulated expression in combination with a cardiac-specific tTA-expressing transgene (34). Bcl-2 transgenic mice were described previously (36). *Ppif*-targeted mice were also described previously (26), as were *Mlp*$^{-/-}$ mice (67). TAC was performed as previously described by us (45). Doxorubicin was given by i.p injection at 15 mg/kg, and mice were followed for 2 weeks. To quantify necrotic myocytes, 100 μg of mAb against cardiac myosin (Biogenesis) was injected i.v. followed by analysis 24 hours afterward by immunohistochemistry on frozen 7-μm sections with Alexa Fluor–conjugated anti-mouse antibody (Invitrogen). Experiments involving animals were approved by the Institutional Animal Care and Use Committee of Cincinnati Children's Hospital.

Western blot and RT-PCR analyses. Ventricle samples from mouse hearts were frozen in liquid nitrogen and stored at –70°C. For Western blot analysis, heart samples were homogenized in extraction buffer [100 mM $(NH_4)_2SO_4$; 20 mM Tris-HCl, pH 7.5; 10% glycerol; 1% Triton X; 1 mM DTT; 1 mM EDTA; 1 mM EGTA; 10 μM calpain inhibitor II (Roche); and 1 μg/ml pepstatin] and a protease inhibitor cocktail (Complete EDTA-free; Roche) and centrifuged at 3,000 *g* for 5 minutes at 4°C, and the resultant supernatants were saved. Proteins were also analyzed by Western blotting from heart tissue prepared in a sucrose-based buffer (250 mM sucrose; 10 mM Tris-HCl, pH 7.5; 1 mM DTT; 1 mM EDTA; and protease inhibitors; Roche). These heart samples were homogenized with a motor-driven teflon homogenizer in sucrose extraction buffer, homogenates were centrifuged at 3,000 *g* for 5 minutes at 4°C, and the resultant supernatant was saved and stored at –70°C until use. Western blotting conditions were described previously (68). Antibodies included β2a subunit (gift from K. Campbell, University of Iowa Carver College of Medicine, Iowa City,

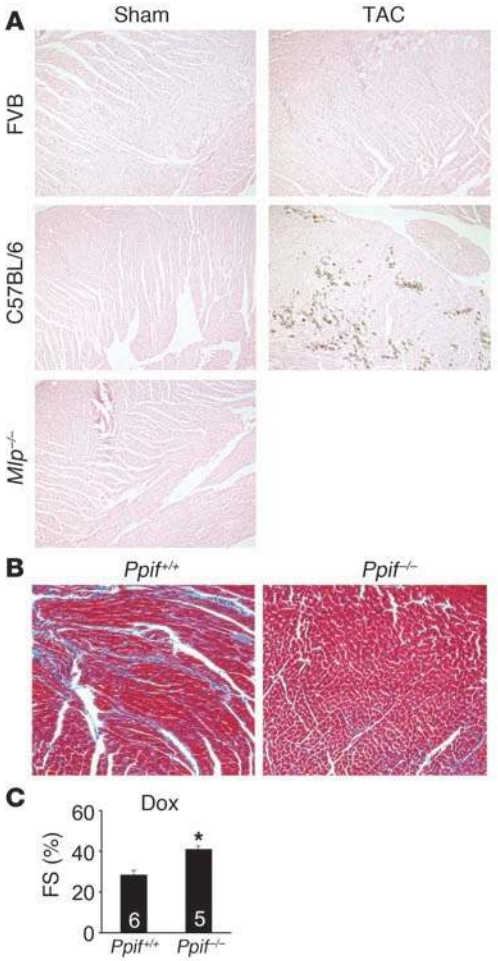

Figure 11
Analysis of necrosis antecedents in other mouse models. (**A**) von Kossa staining from hearts of the indicated mice subjected to sham surgery or TAC. *Mlp*$^{-/-}$ mice were analyzed at baseline, without any surgical intervention. (**B**) Masson's trichrome staining and (**C**) fractional shortening in control *Ppif*$^{+/+}$ and *Ppif*$^{-/-}$ mice 2 weeks after Dox injection (15 mg/kg i.p.). *P < 0.05 versus control, Student's t test. Original magnification, ×100 (**A** and **B**).

USA), α1c subunit, α2δ subunit (Alomone Labs Ltd.), NCX1 (Swant Inc.), SERCA2a, α-tubulin and Bcl-2 (Santa Cruz Biotechnology Inc.), PLN (Affinity BioReagents), and GAPDH (Research Diagnostics). Chemifluorescent detection was performed with the Vistra ECF reagent (Amersham Pharmacia Biotech) and scanned with a Storm 860 PhosphorImager (Molecular Dynamics). RT-PCR was performed as described previously (69).

Histological analysis. Hearts were collected at the indicated times, fixed in 10% formalin–containing PBS, and embedded in paraffin. Serial 7-μm heart sections were cut and stained with H&E and Masson's trichrome. Assessment of TUNEL from paraffin sections was performed as previously described (69) using a TMR Red In Situ Death Detection Kit (Roche). von Kossa staining was performed to detect Ca^{2+} deposits according to the manufacturer's protocol (Diagnostic BioSystems Inc.).

Metamorph analysis. To quantify the damaged/inflamed and fibrotic areas in a cardiac histological section, Metamorph analysis was performed as previously described (70). In brief, Masson's trichrome–stained longitudinal heart sections were photographed using an Olympus U-TVIX digital camera. Images were acquired using SPOT INSIGHT software (Diagnostic Instruments Inc.). For each heart section, 10 photographs were taken at ×200 magnification to represent the entire heart section. Images were analyzed with Metamorph 6.1 software (Universal Imaging Corp.), and the average percent blue area was calculated across at least 3 independent hearts by an investigator blinded to group.

Echocardiography, working heart preparation, and minipump implantation. Mice from all genotypes or treatment groups were anesthetized with isoflurane, and echocardiography was performed using a Hewlett Packard 5500 instrument with a 15-MHz microprobe as previously described (45). Echocardiographic measurements were taken on M-mode in triplicate for each mouse. The isolated work-performing heart preparation from mice was described in detail previously (71). Alzet mini-osmotic pumps (no. 2002; Alza Corp.) containing either Iso (60 mg/kg/d) or PBS were surgically inserted dorsally and subcutaneously in mice under isoflurane anesthesia. All surviving mice were analyzed by echocardiography and sacrificed 2 weeks later.

Drug treatment. To shut down β2a protein expression in DTG mice, Dox (Sigma-Aldrich) was administered at 1 g/l in the drinking water for 2–3 weeks. The Ca^{2+} channel antagonist verapamil (Sigma-Aldrich) was given at 0.1 mg/ml (roughly 10 mg/kg/d) in the drinking water as previously reported (72). The β-adrenergic receptor antagonist metoprolol (Sigma-Aldrich) was also given in the drinking water at 2 g/ml as previously reported (73).

Ca^{2+} current measurements and cell shortening. Ventricular myocytes were isolated as described previously (74). Myocytes were maintained at room temperature in 5% CO_2, and 95% O_2 and used within 8 hours of isolation. Myocytes were placed in a chamber mounted on an inverted Nikon microscope and perfused with normal physiological solution (Tyrode) containing 1 mM Ca^{2+}. Contractions were measured with video edge detector (35). Adenoviral infection with β2a or GFP adenoviruses was described previously (35). Intracellular Ca^{2+} was measured with either Fluo-4 or Indo-1 as described previously (35, 75). Whole-cell Ca^{2+} ($[Ca^{2+}]_o$, 2 mM) current was recorded as described previously (35). NCX current was measured as described by Wei et al. (76).

Statistics. All results are presented as means ± SEM. Statistical analysis was performed using InStat 3.0 software (GraphPad Software) for all unpaired Student's t tests. Prism 3.0 software was used for ANOVA (GraphPad Software). All tests were performed as described in the figure legends. A P values of less than 0.05 was considered significant.

Acknowledgments

This work was supported by the National Institutes of Health (to J.D. Molkentin). H. Nakayama was supported by a Post-Doctoral Fellowship from the Ohio Valley Affiliate branch of the American Heart Association (0425386B). J.D. Molkentin is an Established Investigator of the American Heart Association. This work was also supported by an international collaborative research grant in cardiovascular disease from the Leducq Fondation.

Received for publication November 26, 2006, and accepted in revised form May 14, 2007.

Address correspondence to: Jeffery D. Molkentin, Cincinnati Children's Hospital Medical Center, Molecular Cardiovascular Biology, 3333 Burnet Ave. MLC 7020, Cincinnati, Ohio 45229, USA. Phone: (513) 636-3557; Fax (513) 636-5958; E-mail: jeff.molkentin@cchmc.org. Or to: Steven R. Houser, Department of Physiology, Temple University School of Medicine, 3400 N. Broad St., Philadelphia, Pennsylvania 19140, USA. Phone: (215) 707-3278; Fax: (215) 707-0170; E-mail: srhouser@temple.edu.

Hiroyuki Nakayama and Xiongwen Chen contributed equally to this work.

1. Hobbs, R.E. 2004. Guidelines for the diagnosis and management of heart failure. *Am. J. Ther.* **11**:467–472.
2. Levy, D., et al. 2002. Long-term trends in the incidence of and survival with heart failure. *N. Engl. J. Med.* **347**:1397–1402.
3. Zannad, F., et al. 1999. Incidence, clinical and etiologic features, and outcomes of advanced chronic heart failure: the EPICAL Study. Epidemiologie de l'Insuffisance Cardiaque Avancee en Lorraine. *J. Am. Coll. Cardiol.* **33**:734–742.
4. Haldeman, G.A., Croft, J.B., Giles, W.H., and Rashidee, A. 1999. Hospitalization of patients with heart failure: National Hospital Discharge Survey, 1985 to 1995. *Am. Heart. J.* **137**:352–360.
5. Malek, M. 1999. Health economics of heart failure. *Heart.* **82**(Suppl. 4):IV11–IV13.
6. Lloyd-Jones, D.M., et al. 2002. Lifetime risk for developing congestive heart failure: the Framingham Heart Study. *Circulation.* **106**:3068–3072.
7. Adams, K.F., Jr. 2001. New epidemiologic perspectives concerning mild-to-moderate heart failure. *Am. J. Med.* **110**(Suppl. 7A):6S–13S.
8. Remme, W.J. 2001. Positive inotropes — a new horizon or still a dead end? *Cardiovasc. Drugs Ther.* **15**:375–377.
9. Felker, G.M., and O'Connor, C.M. 2001. Inotropic therapy for heart failure: an evidence-based approach. *Am. Heart J.* **142**:393–401.
10. Goldspink, D.F., Burniston, J.G., and Tan, L.B. 2003. Cardiomyocyte death and the ageing and failing heart. *Exp. Physiol.* **88**:447–458.
11. Colucci, W.S., Sawyer, D.B., Singh, K., and Communal, C. 2000. Adrenergic overload and apoptosis in heart failure: implications for therapy. *J. Card. Fail.* **6**:1–7.
12. Foo, R.S., Mani, K., and Kitsis, R.N. 2005. Death begets failure in the heart. *J. Clin. Invest.* **115**:565–571. doi:10.1172/JCI200524569.
13. Packer, M. 2001. Current role of beta-adrenergic blockers in the management of chronic heart failure. *Am. J. Med.* **110**(Suppl. 7A):81S–94S.
14. Bristow, M.R. 2000. Beta-adrenergic receptor blockade in chronic heart failure. *Circulation.* **101**:558–569.
15. Bouzamondo, A., Hulot, J.S., Sanchez, P., Cucherat, M., and Lechat, P. 2001. Beta-blocker treatment in heart failure. *Fundam. Clin. Pharmacol.* **15**:95–109.
16. , Houser, S.R., Piacentino, V., 3rd, and Weisser, J. 2000. Abnormalities of calcium cycling in the hypertrophied and failing heart. *J. Mol. Cell. Cardiol.* **32**:1595–1607.
17. MacLennan, D.H., and Kranias, E.G. 2003. Phospholamban: a crucial regulator of cardiac contractility. *Nat. Rev. Mol. Cell Biol.* **4**:566–577.
18. Bodi, I., Mikala, G., Koch, S.E., Akhter, S.A., and Schwartz, A. 2005. The L-type calcium channel in the heart: the beat goes on. *J. Clin. Invest.* **115**:3306–3317. doi:10.1172/JCI27167.
19. Pogwizd, S.M., and Bers, D.M. 2004. Cellular basis of triggered arrhythmias in heart failure. *Trends Cardiovasc. Med.* **14**:61–66.
20. Zhang, T., Miyamoto, S., and Brown, J.H. 2004. Cardiomyocyte calcium and calcium/calmodulin-dependent protein kinase II: friends or foes? *Recent Prog. Horm. Res.* **59**:141–168.
21. Kajstura, J., et al. 1996. Necrotic and apoptotic myocyte cell death in the aging heart of Fischer 344 rats. *Am. J. Physiol.* **271**:H1215–H1228.
22. Danial, N.N., and Korsmeyer, S.J. 2004. Cell death: critical control points. *Cell.* **116**:205–219.
23. Zamzami, N., and Kroemer, G. 2001. The mitochondrion in apoptosis: how Pandora's box opens. *Nat. Rev. Mol. Cell Biol.* **2**:67–71.
24. Crompton, M., Barksby, E., Johnson, N., and Capano, M. 2002. Mitochondrial intermembrane junctional complexes and their involvement in cell death. *Biochimie.* **84**:143–152.
25. Halestrap, A.P. 2006. Calcium, mitochondria and reperfusion injury: a pore way to die. *Biochem. Soc. Trans.* **34**:232–237.
26. Baines, C.P., et al. 2005. Loss of cyclophilin D reveals a critical role for mitochondrial permeability transition in cell death. *Nature.* **434**:658–662.
27. Nakagawa, T., et al. 2005. Cyclophilin D-dependent mitochondrial permeability transition regulates some necrotic but not apoptotic cell death. *Nature.* **434**:652–658.
28. Schinzel, A.C., et al. 2005. Cyclophilin D is a component of mitochondrial permeability transition and mediates neuronal cell death after focal cerebral ischemia. *Proc. Natl. Acad. Sci. U. S. A.* **102**:12005–12010.
29. Wagner, J.A., et al. 1989. Alterations in calcium antagonist receptors and sodium-calcium exchange in cardiomyopathic hamster tissues. *Circ. Res.* **65**:205–214.
30. Chen, X., et al. 2002. L-type Ca2+ channel density and regulation are altered in failing human ventricular myocytes and recover after support with mechanical assist devices. *Circ. Res.* **91**:517–524.
31. Schroder, F., et al. 1998. Increased availability and open probability of single L-type calcium channels from failing compared with nonfailing human ventricle. *Circulation.* **98**:969–976.
32. Hullin, R., et al. 2003. Cardiac L-type calcium channel beta-subunits expressed in human heart have differential effects on single channel characteristics. *J. Biol. Chem.* **278**:21623–21630.
33. Chien, A.J., et al. 1995. Roles of a membrane-localized beta subunit in the formation and targeting of functional L-type Ca2+ channels. *J. Biol. Chem.* **270**:30036–30044.
34. Sanbe, A., et al. 2003. Reengineering inducible cardiac-specific transgenesis with an attenuated myosin heavy chain promoter. *Circ. Res.* **92**:609–616.
35. Chen, X., et al. 2005. Ca2+ influx-induced sarcoplasmic reticulum Ca2+ overload causes mitochondrial-dependent apoptosis in ventricular myocytes. *Circ. Res.* **97**:1009–1017.
36. Chen, Z., Chua, C.C., Ho, Y.S., Hamdy, R.C., and Chua, B.H. 2001. Overexpression of Bcl-2 attenuates apoptosis and protects against myocardial I/R injury in transgenic mice. *Am. J. Physiol. Heart Circ. Physiol.* **280**:H2313–H2320.
37. Brocheriou, V., et al. 2000. Cardiac functional improvement by a human Bcl-2 transgene in a mouse model of ischemia/reperfusion injury. *J. Gene Med.* **2**:326–333.
38. Weisleder, N., Taffet, G.E., and Capetanaki, Y. 2004. Bcl-2 overexpression corrects mitochondrial defects and ameliorates inherited desmin null cardiomyopathy. *Proc. Natl. Acad. Sci. U. S. A.* **101**:769–774.
39. Trafford, A.W., Diaz, M.E., O'Neill, S.C., and Eisner, D.A. 2002. Integrative analysis of calcium signalling in cardiac muscle. *Front. Biosci.* **7**:d843–d852.
40. Vassalle, M., and Lin, C.I. 2004. Calcium overload and cardiac function. *J. Biomed. Sci.* **11**:542–565.
41. Henderson, S.A., et al. 2004. Functional adult myocardium in the absence of Na+-Ca2+ exchange: cardiac-specific knockout of NCX1. *Circ. Res.* **95**:604–611.
42. Reuter, H., et al. 2003. Cardiac excitation-contraction coupling in the absence of Na(+) - Ca2+ exchange. *Cell Calcium.* **34**:19–26.
43. Muth, J.N., Bodi, I., Lewis, W., Varadi, G., and Schwartz, A. 2001. A Ca(2+)-dependent transgenic model of cardiac hypertrophy: a role for protein kinase Calpha. *Circulation.* **103**:140–147.
44. Yasuda, S., et al. 2005. Dystrophic heart failure blocked by membrane sealant poloxamer. *Nature.* **436**:1025–1029.
45. Nakayama, H., Wilkin, B.J., Bodi, I., and Molkentin, J.D. 2006. Calcineurin-dependent cardiomyopathy is activated by TRPC in the adult mouse heart. *FASEB J.* **20**:1660–1670.
46. Kuwahara, K., et al. 2006. TRPC6 fulfills a calcineurin signaling circuit during pathologic cardiac remodeling. *J. Clin. Invest.* **116**:3114–3126. doi:10.1172/JCI27702.
47. Ai, X., Curran, J.W., Shannon, T.R., Bers, D.M., and Pogwizd, S.M. 2005. Ca2+/calmodulin-dependent protein kinase modulates cardiac ryanodine receptor phosphorylation and sarcoplasmic reticulum Ca2+ leak in heart failure. *Circ. Res.* **97**:1314–1322.
48. Marx, S.O., et al. 2000. PKA phosphorylation dissociates FKBP12.6 from the calcium release channel (ryanodine receptor): defective regulation in failing hearts. *Cell.* **101**:365–376.
49. Wehrens, X.H., et al. 2003. FKBP12.6 deficiency and defective calcium release channel (ryanodine receptor) function linked to exercise-induced sudden cardiac death. *Cell.* **113**:829–840.
50. Slack, J.P., et al. 2001. The enhanced contractility of the phospholamban-deficient mouse heart persists with aging. *J. Mol. Cell. Cardiol.* **33**:1031–1040.
51. Yano, M., Ikeda, Y., and Matsuzaki, M. 2005. Altered intracellular Ca^{2+} handling in heart failure. *J. Clin. Invest.* **115**:556–564. doi:10.1172/JCI200524159.
52. Fatkin, D., et al. 2000. An abnormal Ca^{2+} response in mutant sarcomere protein-mediated familial hypertrophic cardiomyopathy. *J. Clin. Invest.* **106**:1351–1359.
53. Semsarian, C., et al. 2002. The L-type calcium channel inhibitor diltiazem prevents cardiomyopathy in a mouse model. *J. Clin. Invest.* **109**:1013–1020. doi:10.1172/JCI200214677.
54. Engelhardt, S., Hein, L., Wiesmann, F., and Lohse, M.J. 1999. Progressive hypertrophy and heart failure in beta1-adrenergic receptor transgenic mice. *Proc. Natl. Acad. Sci. U. S. A.* **96**:7059–7064.
55. Liggett, S.B., et al. 2000. Early and delayed consequences of beta(2)-adrenergic receptor overexpression in mouse hearts: critical role for expression level. *Circulation.* **101**:1707–1714.
56. Engelhardt, S., et al. 2001. Early impairment of calcium handling and altered expression of junctin in hearts of mice overexpressing the beta1-adrenergic receptor. *FASEB J.* **15**:2718–2720.
57. Mialet Perez, J., et al. 2003. Beta 1-adrenergic receptor polymorphisms confer differential function and predisposition to heart failure. *Nat. Med.* **9**:1300–1305.
58. Schwarz, B., et al. 2003. Altered calcium transient and development of hypertrophy in beta2-adrenoceptor overexpressing mice with and without pressure overload. *Eur. J. Heart Fail.* **5**:131–136.
59. Engelhardt, S., et al. 2004. Altered calcium handling is critically involved in the cardiotoxic effects of chronic beta-adrenergic stimulation. *Circulation.* **109**:1154–1160.
60. Wencker, D., et al. 2003. A mechanistic role for cardiac myocyte apoptosis in heart failure. *J. Clin. Invest.* **111**:1497–1504. doi:10.1172/JCI200317664.
61. Zhang, T., et al. 2003. The deltaC isoform of CaMKII is activated in cardiac hypertrophy and induces dilated cardiomyopathy and heart failure. *Circ. Res.* **92**:912–919.
62. Maier, L.S., et al. 2003. Transgenic CaMKIIdeltaC overexpression uniquely alters cardiac myocyte Ca2+ handling: reduced SR Ca2+ load and activated SR Ca2+ release. *Circ. Res.* **92**:904–911.
63. Zhu, W.Z., et al. 2003. Linkage of β1-adrenergic stimulation to apoptotic heart cell death through protein kinase A–independent activation of Ca^{2+}/calmodulin kinase II. *J. Clin. Invest.* **111**:617–625. doi:10.1172/JCI200316326.
64. Grueter, C.E., et al. 2006. L-type Ca2+ channel facilitation mediated by phosphorylation of the beta subunit by CaMKII. *Mol. Cell.* **23**:641–650.
65. Kim, J.S., Jin, Y., and Lemasters, J.J. 2006. Reactive oxygen species, but not Ca2+ overloading, trigger pH- and mitochondrial permeability transition-dependent death of adult rat myocytes after ischemia-reperfusion. *Am. J. Physiol. Heart Circ. Physiol.* **290**:H2024–H2034.

66. Bueno, O.F., et al. 2004. Calcineurin Abeta gene targeting predisposes the myocardium to acute ischemia-induced apoptosis and dysfunction. *Circ. Res.* **94**:91–99
67. Arber, S., et al. 1997. MLP-deficient mice exhibit a disruption of cardiac cytoarchitectural organization, dilated cardiomyopathy, and heart failure. *Cell.* **88**:393–403.
68. De Windt, L.J., Lim, H.W., Haq, S., Force, T., and Molkentin, J.D. 2000. Calcineurin promotes protein kinase C and c-Jun NH2-terminal kinase activation in the heart. Cross-talk between cardiac hypertrophic signaling pathways. *J. Biol. Chem.* **275**:13571–13579.
69. Oka, T., et al. 2006. Cardiac-specific deletion of Gata4 reveals its requirement for hypertrophy, compensation, and myocyte viability. *Circ. Res.* **98**:837–845.
70. Parsons, S.A., Millay, D.P., Sargent, M.A., McNally, E.M., and Molkentin, J.D. 2006. Age-dependent effect of myostatin blockade on disease severity in a murine model of limb-girdle muscular dystrophy. *Am. J. Pathol.* **168**:1975–1985.
71. Gulick, J., et al. 1997. Transgenic remodeling of the regulatory myosin light chains in the mammalian heart. *Circ. Res.* **80**:655–664.
72. Oudit, G.Y., et al. 2003. L-type Ca2+ channels provide a major pathway for iron entry into cardiomyocytes in iron-overload cardiomyopathy. *Nat. Med.* **9**:1187–1194.
73. Harding, V.B., Jones, L.R., Lefkowitz, R.J., Koch, W.J., and Rockman, H.A. 2001. Cardiac beta ARK1 inhibition prolongs survival and augments beta blocker therapy in a mouse model of severe heart failure. *Proc. Natl. Acad. Sci. U. S. A.* **98**:5809–5814.
74. Zhou, Y.Y., et al. 2000. Culture and adenoviral infection of adult mouse cardiac myocytes: methods for cellular genetic physiology. *Am. J. Physiol. Heart Circ. Physiol.* **279**:H429–H436.
75. Chen, X., et al. 2007. Adolescent feline heart contains a population of small, proliferative ventricular myocytes with immature physiological properties. *Circ. Res.* **100**:536–544.
76. Wei, S.K., et al. 2003. Protein kinase A hyperphosphorylation increases basal current but decreases beta-adrenergic responsiveness of the sarcolemmal Na+-Ca2+ exchanger in failing pig myocytes. *Circ. Res.* **92**:897–903.